

The Distribution of Bar and Spiral Arm Strengths in Disk Galaxies

R. Buta and S. Vasylyev

Department of Physics and Astronomy, University of Alabama, Box 870324, Tuscaloosa, AL 35487

H. Salo and E. Laurikainen

Division of Astronomy, Department of Physical Sciences, University of Oulu, Oulu, FIN-90014, Finland

ABSTRACT

The distribution of bar strengths in disk galaxies is a fundamental property of the galaxy population that has only begun to be explored. We have applied the bar/spiral separation method of Buta, Block, and Knapen to derive the distribution of maximum relative gravitational bar torques, Q_b , for 147 spiral galaxies in the statistically well-defined Ohio State University Bright Galaxy Survey (OSUBGS) sample. Our goal is to examine the properties of bars as independently as possible of their associated spirals. We find that the distribution of bar strength declines smoothly with increasing Q_b , with more than 40% of the sample having $Q_b \leq 0.1$. In the context of recurrent bar formation, this suggests that strongly-barred states are relatively short-lived compared to weakly-barred or non-barred states. We do not find compelling evidence for a bimodal distribution of bar strengths. Instead, the distribution is fairly smooth in the range $0.0 \leq Q_b < 0.8$.

Our analysis also provides a first look at spiral strengths Q_s in the OSU sample, based on the same torque indicator. We are able to verify a possible weak correlation between Q_s and Q_b , in the sense that galaxies with the strongest bars tend also to have strong spirals.

Subject headings: galaxies: spiral; galaxies: photometry; galaxies: kinematics and dynamics; galaxies: structure

1. Introduction

Bars and spirals are an important part of the morphology of disk galaxies. These “showy disk morphological features which characterize the (Hubble) tuning fork” (Firmani & Avila-Reese 2003) play a role in general classification schemes (e.g., Hubble 1926; Sandage 1961; de Vaucouleurs 1959; Sandage & Bedke 1994), and also can be tied to disk galaxy evolution (e.g., Kormendy & Kennicutt 2004). Over the past two decades, there has been a great deal of interest in the properties of bars, including quantification of bar strength (e.g., Elmegreen & Elmegreen 1985; Martin 1995; Wozniak et al. 1995; Martinet & Friedli 1997; Rozas et al. 1998; Aguerri et al. 1998; Seigar & James 1998; Aguerri 1999; Chapelon et al. 1999; Abraham &

Merrifield 2000; Shlosman et al. 2000; Buta & Block 2001; Laurikainen & Salo 2002; Knapen et al. 2002), bar pattern speeds (Elmegreen et al. 1996; Corsini et al. 2003, 2004; Debattista and Williams 2004; Aguerri et al. 2003; Debattista et al. 2002; Gerssen et al. 1999; Merrifield and Kuijken 1995), mass inflow rates (Quillen et al. 1995), and studies of the distribution of bar strengths (Block et al. 2002; Whyte et al. 2002; Buta, Laurikainen, & Salo 2004). The most recent studies have indicated, on one hand, that bar and spiral strength can be quantified in a reasonable manner from near-infrared images and, on another hand, that such quantifications are useful for probing both bar and spiral evolution.

The distribution of bar strengths is a partic-

ularly important issue. It is well known that as much as 70% of normal bright galaxies are barred at some level (e.g., Eskridge et al. 2002), which suggests that bars might be long-lived features. However, in the presence of gas, bars are not expected to be permanent features of galaxies, but should dissolve in much less than a Hubble time owing to mass inflow into the nuclear region which can build up a central mass concentration and destroy a bar (Pfenniger and Norman 1990). The high frequency of bars has thus led to the idea that bars dissolve and reform many times during a Hubble time (Combes 2004). If this is the case, the distribution of bar strengths will tell us the relative amount of time a galaxy stays in a given bar state (strong, weak, or non-barred; Bournaud & Combes 2002; Block et al. 2002).

Block et al. (2002) and Buta, Laurikainen, & Salo (2004=BLS04) used the gravitational torque method (GTM; Buta & Block 2001; Laurikainen & Salo 2002) to derive maximum relative nonaxisymmetric torque strengths Q_g for the Ohio State University Bright Galaxy Survey (OSUBGS, Eskridge et al. 2002), a statistically well-defined sample of nearby bright galaxies. Block et al. (2001, 2004), BLS04, and Laurikainen, Salo, & Rautiainen (2002) showed that Q_g correlates with deprojected bar ellipticity, a popular parameter suggested by Athanassoula (1992) to be a useful (although incomplete) measure of bar strength (e.g., Martin 1995; Whyte et al. 2002). The correlation was found by Laurikainen, Salo, & Rautiainen (2002) to be much better when objectively-measured near-IR ellipticities are used as opposed to the optical ellipticities estimated by Martin (1995) from blue light photographs. The good correlation is very important, because the shape of the bar relates to the shape of the orbits which build up the bar, which should depend on the global force field. Also, BLS04 found that Q_g correlates well with the bar ellipticity parameter f_{bar} measured by Whyte et al. (2002). Q_g is a bar strength indicator that is sensitive to the mass of the bar, and as such should be a better measure of bar strength than bar ellipticity. However, Q_g is affected also by spiral arm torques which can dominate over the torques due to weak bars. Thus, Q_g alone cannot tell us the actual distribution of bar strengths, but only the distribution for stronger bars.

One way to derive the distribution of real bar strengths is to remove the spiral contribution to Q_g . Buta, Block, and Knapen (2003=BBK03) developed a Fourier-based method of separating bars from spirals that utilizes a symmetry assumption (section 3). Block et al. (2004) applied this method to deep near-IR images of 17 bright galaxies to derive true bar strengths Q_b and spiral strengths Q_s . This analysis detected a possible correlation between Q_b and Q_s in the sense that among bars having $Q_b > 0.3$, spiral strength increases with increasing bar strength. Block et al. suggested that the apparent correlation implies that for stronger bars, the bar and the spiral grow together and have the same pattern speed.

Our goal with the present paper is to apply the BBK03 method to nearly 150 spiral galaxies in the OSUBGS, a database of H -band ($1.65\mu\text{m}$) images that have enough depth of exposure to allow reliable Fourier analyses. In the H -band, the extinction is only 19% that in the V -band (Cardelli, Clayton, & Mathis 1989), and such images are suitable for the derivation of gravitational potentials using fast-Fourier transform techniques (Quillen, Frogel, and González 1994; Salo et al. 1999; Laurikainen & Salo 2002). From the separated images, we derive the distributions of bar and spiral strengths and investigate what these tell us about disk galaxies. We also further investigate the correlation between Q_b and Q_s .

2. Galaxy Sample

Our sample consists of 147 bright galaxies drawn from the same sample as used by BLS04, Laurikainen, Salo, and Buta (2004a=LSB04), and Laurikainen et al. (2004b=LSBV04). These previous studies used 180 galaxies, including 158 OSUBGS galaxies having total magnitudes $B_T < 12.0$, $D_{25} < 6''.5$, $0 \leq T \leq 9$, inclination $< 65^\circ$, and $-80^\circ < \delta < +50^\circ$. In addition, this sample included 22 galaxies from the Two Micron All-Sky Survey (2MASS, Skrutskie et al. 1997) which satisfy similar criteria as the OSUBGS but are larger than the $6''.5$ diameter limit. However, the 2MASS images are sufficiently underexposed that they proved inadequate for bar/spiral separation. Whereas bars are detected fairly well in such images, the spirals and background disks are often too faint to characterize reliably, and we do not

use these images further in this paper.

Figure 1 shows that our subset of 147 OSUBGS galaxies is dominated mainly by Sbc and Sc galaxies. The base OSU sample is typical of the bright galaxy population, as shown by Eskridge et al. (2002) and Whyte et al. (2002). BLS04 and LSB04 showed that their OSUBGS/2MASS sample is biased mainly against inclusion of very late-type, low luminosity barred spirals and low surface brightness galaxies. Our subset of 147 galaxies has a similar bias.

3. The BBK03 Technique

The bar/spiral separation method of BBK03 depends on a simple assumption concerning the behavior of the relative Fourier intensity amplitudes as a function of radius in a bar: the relative intensities decline past a maximum in the same or a similar manner as they rose to that maximum. This is known as the *symmetry assumption*. In a complicated bar and spiral system, only the rising portion of the symmetric curve is seen, as in BBK03's example of NGC 6951, and the symmetry assumption allows the extrapolation of the bar into the spiral region. The assumption is justified from studies of barred galaxies lacking strong spiral structure. BBK03 used the study of 6 barred galaxies from Ohta et al. (1990) and the case of NGC 4394 from the OSUBGS to justify the assumption. The assumption has found further support in studies of SB0 and SB0/a galaxies from the Near-Infrared S0 Survey (Buta et al. 2005; see Buta 2004 for a preliminary summary of these results). In these cases, the bars in the near-infrared are observed against only bulge and disk components, so that the bar is the only significant non-axisymmetric contribution. Since we cannot know *a priori* the form of any particular bar, we judge the effectiveness of a given bar/spiral separation by examining bar plus disk and spiral plus disk intensity maps (see BBK03). If the bar length is underestimated or overestimated, we can detect the failure as positive or negative residuals in the spiral plus disk image.

4. Application of the BBK03 technique to the OSUBGS Sample

The application of the BBK03 technique to the OSUBGS sample required a number of modifica-

tions. First, the method was developed using deep K_s images with pixel sizes of $0''.24$ (Block et al. 2004). In contrast, the OSUBGS H -band images have pixel sizes ranging from $1''.11$ to $1''.50$ and are noisier at large radii than the K_s images used by Block et al. (2004). These two factors complicate separation, but the pixel size problem could be handled effectively by resampling the images into pixels one-quarter as large using IRAF routine IMLINTRAN.

In our analysis of the OSUBGS sample, we encountered a greater range of complications in the relative Fourier intensity curves, such as multiple bars and the effects of decomposition errors on central isophotes. Thus, it was necessary to adapt the BBK03 method to deal with the new complications. The effects of decomposition errors were particularly serious. For all separations, we used deprojected images based on bulge/disk/bar decompositions from LSBV04. In each case, the bulge was assumed to be spherical, but in those cases where the assumption may be wrong, the decomposition led to symmetric regions of lower intensity on each side of the center where too much bulge light was subtracted. In about a dozen cases, the problem was sufficiently serious that bar/spiral separation could not be carried out. In most cases, the problem could be treated in a two-step separation process, which also proved very effective for cases with multiple bars or ovals.

Figure 2 shows the lower-order Fourier representations used to separate the bars and spirals in 24 OSUBGS galaxies. These objects illustrate well the types of extrapolations needed to deal with the wide range of bar types found in the sample. While for many (e.g., NGC 289, 864, 1637, 3261, 3686, 4027, 4254, 4303, 4548, 4995, 5085, 5483, 5921, and 6300) the symmetry assumption appears to work well, for others (e.g., NGC 613, 1087, 4457, 4579, 4593, and the higher order terms for NGC 3261 and 4548) we found it effective to fit a single gaussian to the rising relative intensities (or even a double gaussian, as in NGC 1087). We also followed the procedure of BBK03 to extrapolate the bars as little as possible, so that if the observed relative Fourier amplitudes due to the bar could be detected beyond the maximum, as much as possible of the decline is used as observed. Two cases shown in Figure 2 are NGC 1559 and NGC 2964.

It is likely that some bar profiles are indeed gaussian in nature, although the physical implication of such a representation is not explored here. Some profiles are symmetric but not necessarily gaussian (e.g., NGC 1637) or are clearly asymmetric (as in NGC 1087, 1559, and 2964). The effectiveness of the separations of the 24 galaxies are shown in Figure 3. In general, very good separations are possible by the BBK03 procedure. The partly gaussian-fitted bar representation for NGC 4548 has cleanly removed the bar with little residual bar light remaining. In NGC 4579, gaussian fits to all the main bar Fourier terms allows the inner part of the spiral to be more clearly seen. The complex bar in NGC 1087, represented by two non-coincident gaussians, is well-separated from the complex spiral which itself appears to be affected by considerable star formation. This bar does not follow the symmetry assumption, except for the individual gaussian components.

In many of the bar images, ring-like structures, sometimes slightly oval and sometimes weakly spiral, are seen. These rings in large part represent the axisymmetric component of the associated spirals. Also, some failure of the bar extrapolations can cause these weak structures. In the spiral images also, one often sees a filling in of the inner part of the pattern. This is due to the axisymmetric part of the bar. Maximum relative gravitational torques must be calculated against the total axisymmetric background, including whatever contributions the spirals and bars themselves make to this background.

BBK03 noted that in some bars where the spiral is weak or absent, the maxima of the higher order bar terms shift towards larger radii (e.g., Ohta et al. 1990). These shifts are sometimes seen in our bar representations, but in many cases there is little or no shift detectable. Also, Figure 1 shows that our bar representation for NGC 4593 has fitted peaks in $m=4$ and 6 at smaller radii than for $m=2$.

The symmetry assumption leads to double-humped bar profiles in the strong bars of NGC 1300 and NGC 5921. In both of these cases, the bar image includes a weak elongated ring pattern that contributes little to the torques. In both cases also, the spiral plus disk image looks reasonably bar-free, but a slight asymmetry in the bar leaves a small residual bar spot on the lower right end of

the bar in NGC 5921.

Separation was especially effective for inner ovals. Small ovals in NGC 4254, 5085, 5247, 5248, and 5483 were easily mapped and removed with just a few terms. In the case of NGC 5085, we used the symmetry assumption twice, one for the inner oval and one for an outer oval (Figure 2s). The bar mapping for NGC 5248 shows a double-humped profile that could in principle be represented as a double-gaussian. In a few cases (e.g., NGC 613, 4457, 4579, 4593), the separation successfully removed the primary bar but left a small oval in the center. These ovals tend to be weak compared to the primary bar, and were sometimes left in the spiral plus disk image. In other cases, a two-step process could be used to remove them from the spiral plus disk image, if necessary.

5. Quantitative Bar and Spiral Strengths

We were able to carry out reasonably successful bar/spiral separations for 147 OSUBGS galaxies. The 33 missing objects from the LSBV04 sample include the original 22 2MASS galaxies in their sample and 11 other cases where the decompositions left complex residual structure in the bulge region that prevented a reliable Fourier extrapolation of the bar light.

For the 147 separated galaxies, we computed bar and spiral strengths following LSBV04. Gravitational potentials are inferred from the bar and spiral images assuming a constant mass-to-light ratio. The potentials are derived from Poisson's equation using a fast-Fourier transform technique. A polar grid approach is used to minimize the effects of noise at large radii (e.g., Laurikainen and Salo 2002). Vertical thickness is taken into account using an exponential density function having a scaleheight h_z scaled from the radial scalelength h_R using a type-dependent formulation (de Grijs 1998). For each image, the radial variation, Q_T , of the maximum tangential force relative to the mean background radial force is computed. Then the maximum ratio from the bar image defines Q_b and the radius $r(Q_b)$ and the maximum ratio from the spiral image defines Q_s and $r(Q_s)$. Figure 4 shows a schematic of these definitions, based on NGC 6951 (from BBK03). Since bar/spiral separation uses mainly even Fourier terms for the bar, the procedure leaves the odd

Fourier terms and much of the image noise in the spiral plus disk image. Thus, it was necessary to inspect the plots for the spirals to eliminate spurious maxima due to noise at large radii.

The BBK03 definition of Q_g , shown in Figure 4, differs slightly from that actually used in BLS04, LSB04, and LSBV04, where Q_g was taken to be the maximum Q_T in the bar/oval region when such features were present, and the general maximum Q_T for mostly non-barred spirals. In general, the differences between the formal Q_g defined by BBK03 and that used in the previously cited papers will not be large, but were necessitated by the higher noise level in the OSUBGS images compared to those used by BBK03 and Block et al. (2004).

Table 1 lists the derived parameters for the 147 galaxies. The typical uncertainties in maximum relative gravitational torques are discussed by BBK03, BLS04, and LSBV04. In the present paper, we note that the uncertainty in the constant mass-to-light ratio assumption, as well as the effects of disk truncation, will likely affect Q_b and Q_s differently, because $r(Q_s)$ can significantly exceed $r(Q_b)$, as shown for many cases in Table 1. In BLS04, we showed that the typical dark halo correction to Q_g is about 5% for the galaxies that define the OSUBGS sample, based on a “universal rotation curve” analysis (Persic, Salucci, & Stel 1996). Since $r(Q_g)$ will generally be intermediate between $r(Q_b)$ and $r(Q_s)$, we expect the dark halo contribution affects Q_s more than Q_b . To minimize the effects of disk truncation, we chose a maximum radius (RADMAX) for all calculations of 127 pixels, which is the maximum circle contained in each image. RADMAX is the radius of the zone for which and from which forces are calculated. Laurikainen & Salo (2002) showed that as long as $\text{RADMAX}/r(Q_g) > 2$, disk truncation should not significantly affect the force ratio. In almost all cases, $r(Q_b)$ satisfies this condition, but $r(Q_s)$ may or may not satisfy it. Thus, our derived Q_s values cannot be taken as definitive, but as indicative of the approximate spiral strength. Some Q_s values are also affected by star formation, and in general Q_s is probably overestimated on average in our analysis.

6. Bar/Spiral Strength Correlations

We examine correlations between our measured Q_b and Q_s values and other parameters. Figure 5 shows plots of $\langle Q_b \rangle$ and $\langle Q_s \rangle$ versus RC3 family classification. Figure 5a shows a virtually linear correlation between $\langle Q_b \rangle$ and RC3 family over all types, verifying that the intermediate de Vaucouleurs family class SAB is justified (see also Block et al. 2001). This is the case even when the sample is divided into types $T \leq 4$ (Figure 5c) and $T > 4$ (Figure 5e). The right panels of Figure 5 show only weaker correlations of $\langle Q_s \rangle$ with bar family. In all three panels, $\langle Q_s \rangle$ is higher for SB galaxies than for SA galaxies. Table 2 summarizes the mean values displayed.

Table 1 also lists the “OSU B ” and “OSU H ” family classifications from Eskridge et al. (2002), based on visual inspection of the OSUBGS B -band and H -band images. Eskridge et al. noted that many galaxies classified as non-barred or weakly barred in RC3 appear more strongly barred in the near-IR. We have computed a “ Q_b family” to compare with these estimates (see Table 3). We define an SA galaxy to be one which has $Q_b < 0.05$, while an SB galaxy is defined to have $Q_b \geq 0.25$. Between these extremes we define classes SAB, SAB, and SAB using the notation of de Vaucouleurs (1963), designed to illustrate the continuity aspect of bar strength. The different Q_b families do not involve equal steps in Q_b : the SB category involves a much broader range of bar strengths than does SA, and we give a broader range to SAB compared to SAB and SAB. Comparison between the Q_b family and the OSU H family shows the two often disagree. Many OSU H SB galaxies end up as Q_b family SAB because the bars are really not that strong. Table 4 summarizes 6 galaxies from Eskridge et al. (2000) noted to have changed classification from SA to SB in going from the B to the H band. However, the Q_b family indicates the bars are still weak, even in the near-IR. Some disagreements occur for cases where the spiral comes off the ends of the bar with a large pitch angle, an example being NGC 1042. In this case, there is an oval that we have interpreted as all or some of the bar for bar/spiral separation.

In other cases, the Q_b family gives an SAB or SAB family for cases which are clearly SB in blue light. Some notable examples are NGC 4643,

5101, and 5701, all early-type spirals. In these cases, the bars are simply not as strong as they appear to be because of the presence of a strong bulge component, which contributes significantly to the axisymmetric background.

Table 5 summarizes a general comparison between the Q_b family and the other sources of bar family classification, including the classification of LSBV04 whereby a “Fourier bar” is defined to be one where the phases of the main $m=2$ and $m=4$ Fourier components are maintained nearly constant in the bar region. The most striking aspect of the RC3 comparison is the number of objects classified as SA in RC3 which have a Q_b family of SAB, meaning some bar or oval was detected in the near-IR. A similar comparison is found for the OSU B classifications, which is not surprising since RC3 families are also based on B -band images. The comparison with the OSU H classifications shows that, as highlighted before, many OSU H SB galaxies have bars that are not that strong, and come out with a Q_b family of SAB. The Fourier bar comparison gives very similar results but requires mainly that the low order Fourier phases be constant, not that the bar should be especially strong.

Figure 6 shows plots of $\langle Q_b \rangle$ and $\langle Q_s \rangle$ versus: (a,b) the extinction- and tilt-corrected absolute blue magnitude M_B^0 based on parameters from RC3 and distances from Tully (1988); (c,d) the extinction and tilt-corrected mean effective blue light surface brightness μ'_{eo} (mag arcmin $^{-2}$; see equation 71 of RC3); and (e,f) de Vaucouleurs revised Hubble-Sandage type, coded on the RC3 numerical scale. Little correlation with absolute magnitude is found, although this is partly due to the fact that the sample is biased against late-type, low luminosity barred spirals (BLS04). Except for the lowest surface brightness bin, there is little correlation between $\langle Q_b \rangle$ and μ'_{eo} , while some correlation between $\langle Q_s \rangle$ and μ'_{eo} is found. The mean spiral strength appears to increase with increasingly fainter surface brightness, changing by more than a factor of two, an effect that may be partly due to star formation and partly due to increased image noise for the lower surface brightness objects. Figure 6e shows the same kind of correlation between $\langle Q_b \rangle$ and type discussed by BLS04 and LSB04 for $\langle Q_g \rangle$, in the sense that maximum relative gravitational

torques are larger for later types. Figure 6f shows the same may be true for spiral strengths as well.

BLS04 and LSB04 attributed the type dependence in Q_g as due to the increased prominence of the bulge in early-type spirals. This rather counterintuitive result, that significant-looking bars in early-types actually have weaker relative torques than those in later types, is due to the fact that what the eye recognizes in photographs as a “bar strength” is the LOCAL SURFACE DENSITY contrast, which is different from the tangential to radial force ratio or its maximum value Q_g . The latter is a global quantity, measuring FORCES from all parts of the galaxy, and should be a more reliable indicator of actual bar strength. This highlights the advantage of the GTM in quantifying bar strength beyond the visual appearance of bars (LSB04). Early-type bars may in fact be more massive and intrinsically stronger than those in later types, but relative to the axisymmetric disks they are imbedded within, late-type bars can be stronger.

Figure 7 shows correlations between $\langle Q_b \rangle$ and $\langle Q_s \rangle$ and $\log R_{25}$, the RC3 logarithmic standard isophotal axis ratio (used as an indicator of inclination), and visually estimated Arm Class (Elmegreen and Elmegreen 1987). Arm Classes (ACs) emphasize the symmetry and continuity of spiral arms, and it is worth investigating whether these might correlate with Q_s . No significant trend of either nonaxisymmetric strength parameter is found with $\log R_{25}$, confirming that there is no systematic bias introduced to the torques due to deprojection corrections. However, we detect a weak correlation between $\langle Q_s \rangle$ and AC in the sense that $\langle Q_s \rangle$ is higher for ACs of 9 and 12 (there are no ACs of types 10 and 11), which include the most symmetric, longest arms, compared to ACs of 1–3, which include the chaotic, fragmented arms seen in flocculent spirals. In spite of the apparent correlation, Q_s is not necessarily a suitable replacement for the AC because there is considerable overlap among the classes and the two parameters measure different aspects of spiral structure.

Finally, Figures 7e,f show $\langle Q_b \rangle$ and $\langle Q_s \rangle$ for SB galaxies as functions of RC3 variety classification: ringed (r), pseudoringed (rs), and spiral-shaped (s). With our direct estimates of bar strength, we can investigate the claim made by

Kormendy & Kennicutt (2004) that SB(r) galaxies have stronger bars than SB(s) galaxies, based on the hydrodynamic simulations of Sanders & Tubbs (1980). Table 2 summarizes $\langle Q_b \rangle$ and $\langle Q_s \rangle$ for the three varieties separated by family. Figure 7e shows that, on average, SB(r) galaxies have weaker bars than SB(s) galaxies, contrary to the conclusion of Kormendy & Kennicutt. In our sample also, SB(rs) galaxies have bars as strong on average as those in SB galaxies. The differences are not that significant owing to the large scatter at each variety. Table 2 shows that the statistics are more uncertain for SA galaxies, which strongly emphasize the (s)-variety, and SAB galaxies, which strongly emphasize the (rs) variety.

7. Distribution of Bar and Spiral Arm Strengths

Figures 8a and b show both differential and cumulative distributions of Q_b , while Figures 8c and d show the same for Q_s , for 147 OSUBGS galaxies. For comparison, the distributions of Q_g values (from LSBV04) for the same galaxies are shown in Figures 8e and f. Figures 8a and b show that when bars are isolated from spirals in galaxy images, the lowest bar strength bins, 0.0-0.05 and 0.05-0.10, fill up considerably over the Q_g bins. More than 40% of the galaxies have bars with $Q_b \leq 0.10$, while only 22% have $Q_g \leq 0.10$. It is clear that weak bars or ovals are often masked by spirals and not detected via the Q_g parameter; these bars are visible in Q_T profiles but have force maxima much lower than those induced by spiral arms in the outer parts of the disks. Thus, Q_g does not give a reliable indication of the relative frequency of weak bars.

For the spirals, the lowest Q_s bin is deficient in galaxies compared to the next highest Q_s bin, which is not unexpected given that the sample excludes S0 galaxies. Most spirals are nevertheless fairly weak, with more than 75% having $Q_s \leq 0.20$.

These parameters allow us to assign all the sample galaxies to bar and spiral strength classes (see Table 1). We follow Buta & Block (2001) to make these assignments. For bar class 0 we include any galaxy having $Q_b < 0.05$, while for spiral class 0 we include any galaxy having $Q_s < 0.05$. For bar class 1 we include galaxies having $0.05 \leq Q_b < 0.15$,

while for spiral class 1 we include galaxies having $0.05 \leq Q_s < 0.15$, etc. Thus, the 0 class for bars and spirals involves a narrower range since Q_b and Q_s cannot be negative as defined. These spiral and bar classes define a quantitative near-infrared classification of bars and spirals and can be incorporated into the dust-penetrated classification scheme of Block & Puerari (1999; see Buta & Block 2001). While bar class may represent a suitable replacement for de Vaucouleurs family classifications, spiral class only distinguishes early and late-type spirals and does not discriminate well between individual T -types (Figure 6f).

8. Correlation Between Q_s and Q_b

Elmegreen & Elmegreen (1985) used bar/interbar and arm/interarm contrasts to show that strong spirals are associated with strong bars. Although the bulk of their correlation is based on only a few galaxies, the implication was that the bars might be driving the spirals. However, Sellwood & Sparke (1988) used numerical simulations to show that bars and spirals might be independent features, with different pattern speeds. Block et al. (2004) applied the BBK03 technique to 17 intermediate to late-type spirals and found some correlation between bar and spiral arm torques, but only for the strongest bars. These authors suggested that in strongly-barred galaxies, the bar and the spiral may be growing together and have the same pattern speed.

Figure 9 shows the correlation between Q_s and Q_b (crosses) for the OSUBGS sample. For comparison, the values from Block et al. (2004) for 17 bright spirals are plotted also. The solid curve shows the medians in Q_s for successive bins of 0.1 in Q_b . The plot shows that the median Q_s increases from 0.1 to 0.30 as Q_b increases from 0.05 to 0.75. The rise agrees with that found by Block et al. (2004) within the uncertainties, and again suggests that at lower bar strengths, spiral and bar strengths are largely uncorrelated, while at stronger bar strengths some correlation may be present. The result is difficult to interpret because the numbers of galaxies decrease significantly with increasing Q_b . Also, Q_b and Q_s have correlated uncertainties, in the sense that if Q_b is overestimated by the separation procedure, then Q_s will be underestimated and vice versa.

These uncertainties could be reduced with better quality images as used by Block et al. (2004). Our results largely support the idea of Sellwood & Sparke (1988) that spirals and bars are independent features, with likely different pattern speeds, at least for $Q_b < 0.3$. This is not definitive, however, because as noted by Block et al. (2004), the frequent alignment of bars and rings, which are often parts of the spiral pattern, implies similar pattern speeds in some cases. For higher bar strengths, some correlation between Q_b and Q_s may be present that can only be confirmed with a larger sample of strongly barred spirals.

9. Discussion

9.1. What Determines Bar Strength?

Bar strength in isolated disk galaxies is thought to be determined largely by the effectiveness with which a bar can transfer angular momentum to other galactic components, such as spiral structure, resonances, live halos, and outer bulge stars (Athanasoula 2003). A bar can get very strong if there is nothing to negate this effect. However, a bar can affect its own evolution by driving gas into the center. This builds up the central mass concentration and can lead to an inner Lindblad resonance (ILR), which will feed angular momentum to the bar. When this happens, the bar’s orbital structure can be destroyed and the bar itself fades away (Norman, Sellwood, & Hasan 1996).

Bar strength in non-isolated galaxies can be affected by tidal interactions (Noguchi 1996; Miwa & Noguchi 1998 and also accretion of gas-rich dwarfs or infalling external gas (Sellwood & Moore 1999; Bournaud & Combes 2002; Combes 2004). Miwa and Noguchi (1998) have argued that which bar-forming mechanism (spontaneous or tidal) dominates depends on the relative importance of the disk and halo. They suggest that spontaneous bars will be important if disks are massive relative to their halo, while tidally-induced bars will dominate if the disks are stable against spontaneous bar formation. Noguchi (1987) suggested that the “exponential” and “flat” bars of Elmegreen & Elmegreen (1985) are distinguished by these same two mechanisms, with the former being spontaneous and the latter being tidally triggered. If gas flow helps to dissolve a bar, an interaction may regenerate a bar if there is little disk gas remain-

ing (Berentzen et al. 2004). If a galaxy accretes substantial external gas, it may be susceptible to multiple or recurring bar episodes (Bournaud & Combes 2002, 2004). Several simulation studies (Athanasoula 2003; Athanasoula & Misiriotis 2002; Miwa & Noguchi 1998; Berentzen et al. 2004) have found a correlation between bar strength and bar pattern speed, in the sense that stronger bars have lower pattern speeds.

These results suggest that bar strength is not a permanent feature of galaxies, but can be highly variable over a Hubble time. Evidence in support of this idea comes from the inverse correlation between central mass concentration and bar ellipticity in a sample of spiral galaxies (Das et al. 2003). Thus, the distribution of bar strengths in galaxies may be influenced by a complex variety of effects: environment, mass distribution, the interstellar medium, and the properties of dark matter halos.

9.2. The Distribution of Bar Strengths: Observations versus Theory

We have shown in this paper that a straightforward Fourier technique can be used to separate bars from spirals, allowing us to examine the distribution of bar strengths in galaxies unaffected by the torques due to spirals. We find a preponderance of low bar strengths that was masked in previous Q_g studies partly because of the effects of spiral arm torques. Q_g is only reliable as a bar strength indicator if the bar is the dominant non-axisymmetric feature in a galactic disk. In cases where the spiral dominates, or where the bar and spiral have comparable strengths, Q_g will be an overestimate of bar strength.

The reason for wanting to look at the distribution of bar strengths alone is Sellwood’s (2000) assertion that “most real bars are not made by the bar instability.” This global dynamical instability was first identified in n -body models that showed that a disk-shaped galaxy having sufficient kinetic energy in ordered rotational motion would be unstable to the formation of a bar (Sellwood 1996 and references therein). The way to avoid the linear instability would be a high central concentration, guaranteeing the existence of an ILR inside the bar. Sellwood (2000) noted that many strong bars, such as those found in galaxies like NGC 1300 and 1433, include small circumnuclear

rings whose presence has been tied to the existence of an ILR region (although the exact locations of the rings may not be coincident with ILR; Regan and Teuben 2003). Sellwood noted that enough barred galaxies showed these features to cast considerable doubt on the bar instability as being the explanation of most bars. Other features of the strong bars that suggest the influence of ILRs are the shapes of offset dust lanes (Athanasoula 1992) and observed gas velocity fields.

Sellwood also brought attention to the results of early high redshift studies (e.g., Abraham et al. 1999) that indicated bars are less frequent for $z > 0.5$, suggesting that bars develop long after the disk formed. However, this conclusion has been refuted by more recent studies (Sheth et al. 2003; Elmegreen, Elmegreen, & Hirst 2004; Jogee et al. 2004), which indicate no significant drop in the bar fraction out to $z \approx 1$. Jogee et al. (2004) present the most comprehensive study of bar fraction as a function of redshift, and found that this fraction is virtually constant at $30\% \pm 6\%$ to $z=1$. The implications of their result are thought to be that cold, unstable disks were already in place by $z=1$, and that bars must survive at least 2 Gyr.

In looking for an alternative to the bar instability, Sellwood (2000) suggested bar growth occurs through an episodic process, where the interaction between a bar and a spiral can add particles to the bar and make it longer, while at the same time reducing the bar’s pattern speed. He suggested that it would be useful to be able to predict the distribution of bar strengths for various bar formation scenarios. Of course, it is also useful to know the observed distribution of bar strengths. The BBK03 method and the OSUBGS have allowed us to consider this for the first time.

The only theoretical predictions of an expected distribution of bar strengths have been made for recurrent bar formation models (Bournaud & Combes 2002). Block et al. (2002) used a preliminary Q_g analysis of the OSUBGS sample to derive an observed distribution, and then used the Bournaud & Combes simulation database to derive a theoretical distribution using as much as possible the same assumptions: constant mass-to-light ratio; exponential vertical density distribution having $h_z = 1/12h_R$; inclusion of spiral torques; bulges assumed as flat as the disks; and dark matter ignored. These authors noted that

the observed Q_g distribution shows a deficiency of low Q_g galaxies and an extended “tail” of high Q_g galaxies. The comparison showed that both characteristics were best explained if galaxies are open systems, accreting enough external gas to double their mass in a Hubble time. The distribution of bar strengths would then mainly tell us the relative amount of time galaxies spend in different bar states (strong, weak, or non-barred). The deficiency of low Q_g galaxies was interpreted as due to the “duty cycle” between bar episodes. That is, accretion prevented most galaxies from spending much time in a perfectly axisymmetric state. Some of the nonaxisymmetric torques could be due to spirals which would also be maintained by accretion.

The refined GTM analysis carried out by BLS04, LSB04, and LSBV04 provided a more reliable distribution of Q_g . BLS04 showed that even with refinements that account properly for bulge shapes, and using improved estimates of h_z that allow for the type dependence of h_z/h_R as well as values of h_R derived from two-dimensional bar/bulge/disk decompositions, the observed distribution of Q_g still shows a deficiency of objects having $Q_g < 0.05$ and an extended tail of high Q_g objects. However, the refined distribution shows more low Q_g values than did the Block et al. (2002) analysis, due to a variety of effects discussed by BLS04.

We find that when spiral torques are removed, the distribution of bar strengths is a relatively smoothly declining function with increasing Q_b . It appears that galaxies spend more time in a relatively weakly-barred or non-barred state than they do in a strongly-barred state. Even in these weakly-barred states, they can have significant spiral torques. The question now is whether gas accretion models can account for the actual distribution of bar strengths rather than simply the distribution of total nonaxisymmetry strengths. In principle, a separation analysis could be made for simulations as for images.

Whyte et al. (2002) analyzed the blue and near-infrared images in the OSUBGS, and derived a quantitative bar strength parameter, f_{bar} , which is a rescaled measure of bar ellipticity (Abraham & Merrifield 2000). For the large and well-defined OSUBGS sample, they derived a distribution of f_{bar} which they claim shows evidence for bimodal-

ity, and argue that the bimodality is likely due to rapid evolution from the SB phase to SA and SAB phases. However, the distribution of Q_b suggests a continuous distribution of bar strengths, with no evidence of bimodality. The two results are not really in disagreement because the evidence for bimodality in f_{bar} is very weak, especially in the plot of f_{bar} versus concentration shown by Whyte et al. (2002). The original evidence was found in this same kind of plot by Abraham & Merrifield (2000). In agreement with our results, Whyte et al. (2002) found that SAB galaxies have values of f_{bar} intermediate between SA and SB galaxies.

10. Conclusions

Using a simple Fourier technique, we have separated the bars and spirals in 147 OSUBGS galaxies, and for the first time derived the distribution of actual bar strengths in disk galaxies. We find that the relative frequency of bars is a declining function of bar strength, with more than 40% of the sample being very weakly-barred or non-barred with $Q_b < 0.1$. The higher frequency of weak bars compared to strong ones suggests that strong bars are either very transient or may require more special conditions, such as an interaction. If, in fact, bars are long-lived, as suggested by the results of high redshift studies (e.g., Jogee et al. 2004), then the observed distribution of bar strengths is telling us that cold, unstable disks preferentially form weak bars.

An important piece of the whole picture of barred galaxies is still missing: SB0 galaxies. Block et al. (2002) suggested that in the absence of gas, bars are very robust and can last a Hubble time. What is the distribution of bar strengths in such galaxies? Our SB0 survey (Buta et al. 2005; Buta 2004) should be able to answer this question.

We thank an anonymous referee for helpful comments on the manuscript. RB and SV acknowledge the support of NSF Grant AST-0205143 to the University of Alabama. EL and HS acknowledge the support of the Academy of Finland, and EL also from the Magnus Ehrnrooth Foundation. SV acknowledges the support of the Academy of Finland during two summer visits to Oulu in 2002 and 2003. Funding for the OSU Bright Galaxy Survey was provided by grants from the National Science Foundation (grants AST-

9217716 and AST-9617006), with additional funding from the Ohio State University.

REFERENCES

- Abraham, R. G. & Merrifield, M. R. 2000, *AJ*, 120, 2835
- Abraham, R. G., Merrifield, M. R., Ellis, R. S., Tanvir, N. R., & Brinchmann, J. 1999, *MNRAS*, 308, 569
- Aguerri, J. A. L. 1999, *A&A*, 351, 43
- Aguerri, J. A. L., Beckman, J. E., & Prieto, M. 1998, *AJ*, 116, 2136
- Aguerri, J. A. L., Debattista, V., and Corsini, E. M. 2003, *MNRAS*, 338, 465
- Athanassoula, E. 1992, *MNRAS*, 259, 328
- Athanassoula, E. 2003, *MNRAS*, 341, 1179
- Athanassoula, E. & Misiriotis, A. 2002, *MNRAS*, 330, 35
- Berentzen, I., Athanassoula, E., Heller, C. H., & Fricke, K.J. 2004, *MNRAS*, 347, 220
- Block, D. L. & Puerari, I. 1999, *A&A*, 342, 627
- Block, D. L., Puerari, I., Knapen, J. H., Elmegreen, B. G., Buta, R., Stedman, S., & Elmegreen, D. M. 2001, *A&A*, 375, 761
- Block, D. L., Bournaud, F., Combes, F., Puerari, I., & Buta, R. 2002, *A&A*, 394, L35
- Block, D. L., Buta, R., Knapen, J. H., Elmegreen, D. M., Elmegreen, B. G., & Puerari, I. 2004, *AJ*, 128, 183
- Bournaud, F. & Combes, F., 2002 *A&A*, 392, 83
- Bournaud, F. & Combes, F., 2004, in *SF2A-2004, Semaine de l'Astrophysique*, F. Combes, D. Barret, T. Contini, F. Meynadier, & L. Pagani, eds., Ed-P Sciences, Conference series
- Buta, R. 2004, in *Penetrating Bars Through Masks of Cosmic Dust, The Hubble Tuning Fork Strikes a New Note*, D. L. Block, I. Puerari, K. C. Freeman, R. Groess, & E. K. Block, eds., Springer, Dordrecht, 101
- Buta, R. & Block, D. L. 2001, *ApJ*, 550, 243
- Buta, R., Block, D. L., & Knapen, J. H. 2003, *AJ*, 126, 1148 (BBK03)
- Buta, R., Laurikainen, E., & Salo, H. 2004, *AJ*, 127, 279 (BLS04)
- Buta, R., Laurikainen, E., Salo, H., Block, D. L., & Knapen, J. H. 2005, in preparation
- Cardelli, J. A., Clayton, G. C., & Mathis, J. S. 1989, *ApJ*, 345, 245
- Chapelon, S., Contini, T., & Davoust, E. 1999, *A&A*, 345, 81
- Combes, F. 2004, in *Penetrating Bars Through Masks of Cosmic Dust, The Hubble Tuning Fork Strikes a New Note*, D. L. Block, I. Puerari, K. C. Freeman, R. Groess, & E. K. Block, eds., Springer, Dordrecht, 57
- Corsini, E. M., et al. 2004, *IAU Symp.* 220, S. Ryder, D. J. Pisano, M. A. Walker, & K. C. Freeman, eds., p. 271
- Corsini, E. M., Debattista, V., & Aguerri, J. A. L. 2003, *ApJ*, 599, 29
- Das, M., et al. 2003, *ApJ*, 582, 190
- Debattista, V., Corsini, E. M., and Aguerri, J. A. L. 2002, *MNRAS*, 332, 65
- Debattista, V. and Williams, T. 2004, *ApJ*, 605, 714
- de Grijs, R. 1998, *MNRAS*, 299, 595
- de Vaucouleurs, G. 1959, *Handbuch der Physik*, 53, 275
- de Vaucouleurs, G. 1963, *ApJS*, 8, 31
- de Vaucouleurs, G. et al. 1991, *Third Reference Catalog of Bright Galaxies (New York: Springer) (RC3)*
- Elmegreen, B. G. & Elmegreen, D. M. 1985, *ApJ*, 288, 438
- Elmegreen, B. G., Elmegreen, D. M., & Hirst, A. C. 2004, *ApJ*, 612, 191
- Elmegreen, B. G., Elmegreen, D. M., Chromey, F. R., Hasselbacher, D. A., & Bissell, B. A. 1996, *AJ*, 111, 2233
- Elmegreen, D. M. & Elmegreen, B. G. 1987, *ApJ*, 314, 3
- Eskridge, P., Frogel, J. A., Pogge, R. W., et al. 2000, *AJ*, 119, 536
- Eskridge, P., Frogel, J. A., Pogge, R. W., et al. 2002, *ApJS*, 143, 73
- Firmani, C. & Avila-Reese, V. 2003, *RMxAC*, 17, 107
- Gerssen, J., Kuijken, K., and Merrifield, M. R. 1999, *MNRAS*, 306, 926
- Hubble, E. 1926, *ApJ*, 64, 321
- Jogee, S. et al. 2004, *ApJ*, 615, L105
- Knapen, J., Pérez-Ramírez, D. & Laine, S. 2002, *MNRAS*, 337, 808
- Kormendy, J. and Kennicutt, R. 2004, *ARAA*, 42, 603

- Laurikainen, E., Salo, H., & Buta, R. 2004a, *ApJ*, 607, 103 (LSB04)
- Laurikainen, E., Salo, H., & Rautiainen, P. 2002, *MNRAS*, 331, 880
- Laurikainen, E. & Salo, H. 2002, *MNRAS*, 337, 1118
- Laurikainen, E., Salo, H., Buta, R., & Vasylyev, S. 2004b, *MNRAS*, 355, 1251 (LSBV04)
- Martin, P. 1995, *AJ*, 109, 2428
- Martinet, L. & Friedli, D. 1997, *A&A*, 323, 363
- Merrifield, M. R. & Kuijken, K. 1995, *MNRAS*, 274, 933
- Miwa, T. and Noguchi, M. 1998, *ApJ*, 499, 149
- Noguchi, M. 1987, *MNRAS*, 228, 635
- Noguchi, M. 1996, in *Barred Galaxies*, IAU Coll. No. 157, R. Buta, D. Crocker, and B. G. Elmegreen, eds., ASP Conf. Ser. 91, p. 339
- Norman, C., Sellwood, J. A., & Hasan, H. 1996, *ApJ*, 462, 114
- Ohta, K., Hamabe, M., & Wakamatsu, K. 1990, *ApJ*, 357, 71
- Persic, M., Salucci, P., & Stel, F. 1996, *MNRAS*, 281, 27
- Pfenniger, D. & Norman, C. A. 1990, *ApJ*, 363, 391
- Quillen, A. C., Frogel, J. A., & González, R. A. 1994, *ApJ*, 437, 162
- Quillen, A. C., Frogel, J. A., Kenney, J. D., Pogge, R. W., & Depoy, D. L., 1995, *ApJ*, 441, 549
- Regan, M. & Elmegreen, D. M. 1997, *AJ*, 114, 965
- Regan, M. & Teuben, P. 2003, *ApJ*, 582, 723
- Rozas, M., Knapen, J. H., & Beckman, J. E. 1998, *MNRAS*, 301, 631
- Salo, H., Rautiainen, P., Buta, R., Purcell, G. B., Cobb, M. L., Crocker, D. A., & Laurikainen, E. 1999, *AJ*, 117, 792
- Sandage, A. R. 1961, *The Hubble Atlas of Galaxies*, Carnegie Inst. of Wash. Publ. No. 618
- Sandage, A. & Bedke, J. S. 1994, *The Carnegie Atlas of Galaxies*, Carnegie Inst. of Wash. Publ. No. 638
- Sanders, R. H. & Tubbs, A. D. 1980, *ApJ*, 235, 803
- Seigar, M. S. & James, P. S. 1998, *MNRAS*, 299, 672
- Sellwood, J. 1996, in *Barred Galaxies*, IAU Coll. No. 157, R. Buta, D. Crocker, and B. G. Elmegreen, eds., ASP Conf. Ser. 91, p. 259
- Sellwood, J. A. 2000, in *Dynamics of Galaxies: From the Early Universe to the Present*, F. Combes, G. A. Mamon, & V. Charmandaris, eds., San Francisco, ASP Conf. Ser. 197, p. 3.
- Sellwood, J. A. & Moore, E. M. 1999, *ApJ*, 510, 125
- Sellwood, J. A. & Sparke, L. S. 1988, *MNRAS*, 231, 25P
- Sheth, K., Regan, M. W., Scoville, N. Z., & Strubbe, L. E. 2003, *ApJ*, 592, 13
- Shlosman, I., Peletier, R. F., & Knapen, J. H. 2000, *ApJ*, 535, L83
- Skrutskie, M. F. et al. 1997, in *The Impact of Large-Scale Near-IR Surveys*, F. Gazon et al., eds., Dordrecht, Kluwer, p.25
- Tully, R. B. 1988, *Nearby Galaxies Catalogue*, Cambridge, Cambridge University Press
- Whyte, L., Abraham, R. G., Merrifield, M. R., Eskridge, P. B., Frogel, J. A., & Pogge, R. W. 2002, *MNRAS*, 336, 1281
- Wozniak, H., Friedli, D., Martinet, L., Martin, P., & Bratschi, P. 1995, *A&AS*, 111, 115

TABLE 1
SUMMARY OF PARAMETERS

Galaxy 1	RC3 family 2	OSU <i>B</i> family 3	OSU <i>H</i> family 4	Q_b 5	Q_s 6	$r(Q_b)$ (arcsec) 7	$r(Q_s)$ (arcsec) 8	bar class 9	spiral class 10	Q_b family 11
NGC 150	SB	SAB	SB	0.475	0.254	23	33	5	3	SB
NGC 157	SAB	SB	SA	0.024	0.323	3	21	0	3	SA
NGC 210	SAB	SA	SB	0.052	0.037	29	63	1	0	SAB
NGC 278	SAB	SA	SA	0.046	0.064	5	19	0	1	SA
NGC 289	SB	SB	SB	0.212	0.089	11	49	2	1	SAB
NGC 428	SAB	SAB	SB	0.254	0.100	19	50	3	1	SB
NGC 488	SA	SA	SA	0.028	0.020	11	40	0	0	SA
NGC 578	SAB	SAB	SB	0.180	0.168	9	37	2	2	SAB
NGC 613	SB	SB	SB	0.298	0.319	39	65	3	3	SB
NGC 685	SAB	SB	SB	0.389	0.157	9	23	4	2	SB
NGC 864	SAB	SAB	SB	0.321	0.134	13	19	3	1	SB
NGC 1042	SAB	SAB	SAB	0.044	0.530	5	21	0	5	SA
NGC 1058	SA	SA	SA	0.129	0.097:	15	...	1	1	SAB
NGC 1073	SB	SB	SB	0.561	0.264	15	29	6	3	SB
NGC 1084	SA	SA	SA	0.038	0.197	5	23	0	2	SA
NGC 1087	SAB	SB	SB	0.428	0.265	5	25	4	3	SB
NGC 1187	SB	SB	SB	0.117	0.183	17	31	1	2	SAB
NGC 1241	SB	SAB	SB	0.181	0.153	11	19	2	2	SAB
NGC 1300	SB	SB	SB	0.524	0.184	57	111	5	2	SB
NGC 1302	SB	SAB	SB	0.061	0.033	17	89	1	0	SAB
NGC 1309	SA	SA	SAB	0.091	0.132	9	15	1	1	SAB
NGC 1317	SAB	SB	SB	0.085	0.031	35	83	1	0	SAB
NGC 1371	SAB	SAB	SAB	0.049	0.109	7	19	0	1	SA
NGC 1385	SB	SB	SB	0.269	0.262	3	31	3	3	SB
NGC 1493	SB	SAB	SB	0.319	0.159	9	19	3	2	SB
NGC 1559	SB	SB	SB	0.328	0.185	5	45	3	2	SB
NGC 1617	SB	SA	SAB	0.034	0.078	7	35	0	1	SA
NGC 1637	SAB	SA	SB	0.193	0.066	11	17	2	1	SAB
NGC 1703	SB	SA	SAB	0.073	0.097	9	23	1	1	SAB
NGC 1792	SA	SA	SA	0.060	0.150	5	31	1	2	SAB
NGC 1832	SB	SAB	SB	0.176	0.131	11	39	2	1	SAB
NGC 2090	SA	SAB	SA	0.087	0.090	9	17	1	1	SAB
NGC 2139	SAB	SB	SB	0.356	0.198	3	21	4	2	SB
NGC 2196	SA	SA	SA	0.069	0.094	7	107	1	1	SAB
NGC 2442	SAB	SB	SB	0.412	0.600:	45	71	4	6	SB
NGC 2559	SB	SAB	SB	0.334	0.169	25	43	3	2	SB
NGC 2566	SB	SB	SB	0.270	0.220	45	79	3	2	SB
NGC 2775	SA	SA	SA	0.037	0.043	11	33	0	0	SA
NGC 2964	SAB	SA	SAB	0.270	0.110	13	24	3	1	SB
NGC 3059	SB	SB	SB	0.533	0.305	8	113:	5	3	SB
NGC 3166	SAB	SA	SB	0.108	0.073	21	77	1	1	SAB
NGC 3169	SA	SA	SA	0.089	0.036	11	113:	1	0	SAB
NGC 3223	SA	SA	SA	0.025	0.047	7	81	0	0	SA
NGC 3227	SAB	SAB	SB	0.151	0.078	21	43	2	1	SAB
NGC 3261	SB	SAB	SB	0.166	0.100	15	30	2	1	SAB
NGC 3275	SB	SB	SB	0.183	0.166	19	102	2	2	SAB
NGC 3319	SB	SB	SB	0.537	0.309	9	75	5	3	SB
NGC 3338	SA	SAB	SAB	0.049	0.076	5	33	0	1	SA
NGC 3423	SA	SA	SA	0.037	0.163	7	63	0	2	SA
NGC 3504	SAB	SB	SB	0.286	0.069	19	33	3	1	SB
NGC 3507	SB	SB	SB	0.188	0.098	13	19	2	1	SAB
NGC 3513	SB	SB	SB	0.521	0.293	13	47	5	3	SB
NGC 3583	SB	SAB	SB	0.170	0.189	9	17	2	2	SAB
NGC 3593	SA	SA	SA	0.151	0.010	7	60	2	0	SAB
NGC 3596	SAB	SA	SAB	0.080	0.200	7	30	1	2	SAB
NGC 3646	SI	SA	SAB	0.081	0.260	5	42	1	3	SAB
NGC 3675	SA	SAB	SB	0.078	0.083	11	49	1	1	SAB

TABLE 1—*Continued*

Galaxy	RC3 family	OSU <i>B</i> family	OSU <i>H</i> family	Q_b	Q_s	$r(Q_b)$ (arcsec)	$r(Q_s)$ (arcsec)	bar class	spiral class	Q_b family
1	2	3	4	5	6	7	8	9	10	11
NGC 3681	SAB	SAB	SB	0.187	0.070	5	19	2	1	SAB
NGC 3684	SA	SAB	SAB	0.086	0.163	3	113	1	2	SAB
NGC 3686	SB	SAB	SB	0.225	0.082	7	15	2	1	SAB
NGC 3726	SAB	SAB	SB	0.212	0.174	17	41	2	2	SAB
NGC 3810	SA	SA	SAB	0.049	0.110	7	11	0	1	SA
NGC 3887	SB	SAB	SB	0.093	0.175	9	23	1	2	SAB
NGC 3893	SAB	SA	SAB	0.122	0.132	9	47	1	1	SAB
NGC 3938	SA	SA	SA	0.022	0.052	11	37	0	1	SA
NGC 3949	SA	SAB	SAB	0.171	0.269	3	17	2	3	SAB
NGC 4027	SB	SB	SB	0.569	0.316	3	19	6	3	SB
NGC 4030	SA	SA	SA	0.020	0.059	5	53	0	1	SA
NGC 4051	SAB	SB	SB	0.097	0.257	23	45	1	3	SAB
NGC 4123	SB	SB	SB	0.331	0.195	21	31	3	2	SB
NGC 4136	SAB	SAB	SB	0.150	0.114	7	17	2	1	SAB
NGC 4138	SA	S	S	0.039	0.035	5	17	0	0	SA
NGC 4145	SAB	SAB	SB	0.427	0.124	3	25	4	1	SB
NGC 4151	SAB	SB	SB	0.114	0.039	43	87	1	0	SAB
NGC 4212	SA	SA	SAB	0.060	0.210	5	19	1	2	SAB
NGC 4242	SAB	SB	SB	0.225	0.050	29	60	2	1	SAB
NGC 4254	SA	SA	SAB	0.098	0.101	9	51	1	1	SAB
NGC 4303	SAB	SB	SB	0.075	0.243	13	27	1	2	SAB
NGC 4314	SB	SB	SB	0.439	0.084	35	61	4	1	SB
NGC 4394	SB	SB	SB	0.259	0.070	21	41	3	1	SB
NGC 4414	SA	SA	SA	0.088	0.143	7	21	1	1	SAB
NGC 4450	SA	SA	SB	0.116	0.085	25	63	1	1	SAB
NGC 4457	SAB	SA	SB	0.078	0.050	19	41	1	1	SAB
NGC 4487	SAB	SAB	SB	0.178	0.070	7	34	2	1	SAB
NGC 4504	SA	SA	SB	0.075	0.138	7	23	1	1	SAB
NGC 4548	SB	SB	SB	0.285	0.155	33	51	3	2	SB
NGC 4571	SA	SA	SA	0.022	0.080	3	30	0	1	SA
NGC 4579	SAB	SB	SB	0.188	0.050	21	49	2	1	SAB
NGC 4580	SAB	SA	SA	0.077	0.088	7	13	1	1	SAB
NGC 4593	SB	SB	SB	0.263	0.104	37	53	3	1	SB
NGC 4618	SB	SB	SB	0.354	0.197	7	67	4	2	SB
NGC 4643	SB	SB	SB	0.245	0.039	27	45	2	0	SAB
NGC 4647	SAB	SB	SB	0.108	0.112	7	57	1	1	SAB
NGC 4651	SA	SA	SAB	0.061	0.095	7	13	1	1	SAB
NGC 4654	SAB	SAB	SB	0.136	0.144	5	45	1	1	SAB
NGC 4665	SB	SB	SB	0.257	0.037	25	73	3	0	SB
NGC 4689	SA	SA	SA	0.050	0.067	13	39	1	1	SAB
NGC 4691	SB	SB	SB	0.499	0.063	9	87	5	1	SB
NGC 4698	SA	SA	SA	0.088	0.059	45	105	1	1	SAB
NGC 4699	SAB	SB	SB	0.138	0.030	9	19	1	0	SAB
NGC 4772	SA	SA	SB	0.042	0.030	45	63	0	0	SA
NGC 4775	SA	SA	SA	0.105	0.125	3	27	1	1	SAB
NGC 4781	SB	SAB	SB	0.205	0.312	7	17	2	3	SAB
NGC 4900	SB	SB	SB	0.372	0.167	5	19	4	2	SB
NGC 4902	SB	SB	SB	0.272	0.060	15	67	3	1	SB
NGC 4930	SB	SB	SB	0.210	0.110	31	109	2	1	SAB
NGC 4939	SA	SAB	SAB	0.119	0.084	11	97	1	1	SAB
NGC 4995	SAB	SAB	SB	0.203	0.207	11	19	2	2	SAB
NGC 5054	SA	SA	SAB	0.065	0.088	13	69	1	1	SAB
NGC 5085	SA	SA	SAB	0.155	0.109	19	43	2	1	SAB
NGC 5101	SB	SB	SB	0.186	0.033	39	109	2	0	SAB
NGC 5121	SA	SA	SA	0.024	0.030	25	57	0	0	SA
NGC 5248	SAB	SA	SA	0.061	0.270	7	51	1	3	SAB
NGC 5247	SA	SA	SA	0.020	0.327	3	65	0	3	SA

TABLE 1—*Continued*

Galaxy	RC3 family	OSU <i>B</i> family	OSU <i>H</i> family	Q_b	Q_s	$r(Q_b)$ (arcsec)	$r(Q_s)$ (arcsec)	bar class	spiral class	Q_b family
1	2	3	4	5	6	7	8	9	10	11
NGC 5334	SB	SB	SB	0.322	0.145	5	11	3	1	SB
NGC 5427	SA	SA	SA	0.083	0.235	7	33	1	2	SAB
NGC 5483	SA	SAB	SB	0.174	0.109	7	19	2	1	SAB
NGC 5643	SAB	SAB	SB	0.321	0.236	27	45	3	2	SB
NGC 5676	SA	SA	SAB	0.087	0.080	11	23	1	1	SAB
NGC 5701	SB	SB	SB	0.139	0.053	27	105	1	1	SAB
NGC 5713	SAB	SAB	SB	0.335	0.111	7	15	3	1	SB
NGC 5850	SB	SB	SB	0.311	0.053	39	65	3	1	SB
NGC 5921	SB	SB	SB	0.255	0.349	21	37	3	3	SB
NGC 5962	SA	SAB	SB	0.141	0.055	9	15	1	1	SAB
NGC 6215	SA	SA	SAB	0.079	0.230	3	24	1	2	SAB
NGC 6221	SB	SAB	SB	0.430	0.207	25	43	4	2	SB
NGC 6300	SB	SAB	SB	0.222	0.175	29	63	2	2	SAB
NGC 6384	SAB	SB	SB	0.135	0.050	11	35	1	1	SAB
NGC 6753	SA	SA	SA	0.029	0.032	5	15	0	0	SA
NGC 6782	SAB	SAB	SB	0.163	0.030	21	44	2	0	SAB
NGC 6902	SA	SA	SB	0.034	0.080	11	30	0	1	SA
NGC 6907	SB	SB	SB	0.071	0.329	3	25	1	3	SAB
NGC 7083	SA	SA	SA	0.033	0.071	5	23	0	1	SA
NGC 7217	SA	SA	SA	0.033	0.036	9	109	0	0	SA
NGC 7205	SA	SA	SAB	0.048	0.061	7	55	0	1	SA
NGC 7213	SA	SA	SA	0.004	0.024	11	93	0	0	SA
NGC 7412	SB	SAB	SAB	0.060	0.434	11	45	1	4	SAB
NGC 7418	SAB	SAB	SB	0.158	0.153	11	35	2	2	SAB
NGC 7479	SB	SB	SB	0.702	0.260	27	41	7	3	SB
NGC 7552	SB	SB	SB	0.393	0.055	39	65	4	1	SB
NGC 7713	SB	SA	SA	0.040	0.097	5	23	0	1	SA
NGC 7723	SB	SB	SB	0.319	0.120	11	22	3	1	SB
NGC 7727	SAB	SAB	SA	0.087	0.145	7	99	1	1	SAB
NGC 7741	SB	SB	SB	0.736	0.324	11	27	7	3	SB
IC 4444	SAB	SA	SB	0.254	0.140	5	16	3	1	SB
IC 5325	SAB	SA	SAB	0.030	0.213	5	11	0	2	SA
ESO 138- 10	SA	SA	SA	0.038	0.134	7	67	0	1	SA

TABLE 2
MEAN BAR AND SPIRAL STRENGTH BY FAMILY AND VARIETY

RC3 classification	$\langle Q_b \rangle$	standard deviation	mean error	$\langle Q_s \rangle$	standard deviation	mean error	n
Full sample							
SA	0.069	0.043	0.006	0.101	0.069	0.010	48
SAB	0.177	0.114	0.017	0.147	0.118	0.018	45
SB	0.294	0.166	0.023	0.171	0.100	0.014	53
$T \leq 4$							
SA	0.062	0.041	0.008	0.082	0.072	0.014	28
SAB	0.143	0.100	0.020	0.134	0.127	0.025	26
SB	0.247	0.131	0.022	0.143	0.101	0.017	36
$T > 4$							
SA	0.080	0.044	0.010	0.127	0.054	0.012	20
SAB	0.225	0.117	0.027	0.165	0.105	0.024	19
SB	0.395	0.191	0.046	0.228	0.069	0.017	17
SA Galaxies							
r	0.047	0.037	0.012	0.066	0.058	0.019	9
rs	0.077	0.025	0.008	0.111	0.034	0.011	9
s	0.074	0.047	0.009	0.109	0.077	0.014	30
SAB Galaxies							
r	0.199	0.094	0.033	0.092	0.056	0.020	8
rs	0.167	0.119	0.022	0.164	0.105	0.020	29
s	0.193	0.124	0.044	0.141	0.189	0.067	8
SB Galaxies							
r	0.201	0.107	0.029	0.135	0.081	0.022	14
rs	0.327	0.139	0.029	0.177	0.093	0.019	23
s	0.329	0.215	0.054	0.193	0.119	0.030	16

TABLE 3
DEFINITIONS OF “ Q_b FAMILIES”

Family	Range
SA	$Q_b < 0.05$
<u>SAB</u>	$0.05 \leq Q_b < 0.10$
SAB	$0.10 \leq Q_b < 0.20$
<u>SAB</u>	$0.20 \leq Q_b < 0.25$
SB	$Q_b \geq 0.25$

TABLE 4
SA GALAXIES CLASSIFIED AS SB IN NEAR-IR BY ESKRIDGE ET AL. (2002)

Name	RC3 Family	OSU H Family	Q_b Family
NGC 3675	SA	SB	<u>S</u> AB
NGC 4450	SA	SB	SAB
NGC 4504	SA	SB	<u>S</u> AB
NGC 5483	SA	SB	SAB
NGC 5962	SA	SB	SAB
NGC 6902	SA	SB	SA

TABLE 5
GENERAL COMPARISON OF Q_b FAMILY WITH OTHER BAR CLASSIFICATIONS

	SA	<u>S</u> AB	SAB	<u>S</u> AB	SB
RC3 SA	21	18	9	0	0
RC3 SAB	5	9	16	3	12
RC3 SB	2	6	9	6	31
OSU B SA	23	23	8	0	2
OSU B SAB	3	6	16	5	9
OSU B SB	1	4	10	4	32
OSU H SA	20	12	3	0	1
OSU H SAB	5	12	4	0	1
OSU H SB	2	9	27	9	41
without Fourier bar	26	23	6	1	2
with Fourier bar	2	10	28	8	41

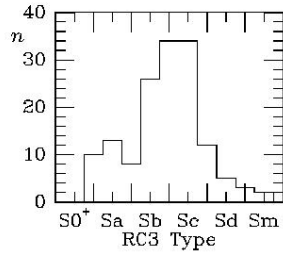


Fig. 1.— Histogram of the distribution of revised Hubble types for the 147 galaxies in our bar/spiral separation sample. The types are from RC3 (de Vaucouleurs et al. 1991).

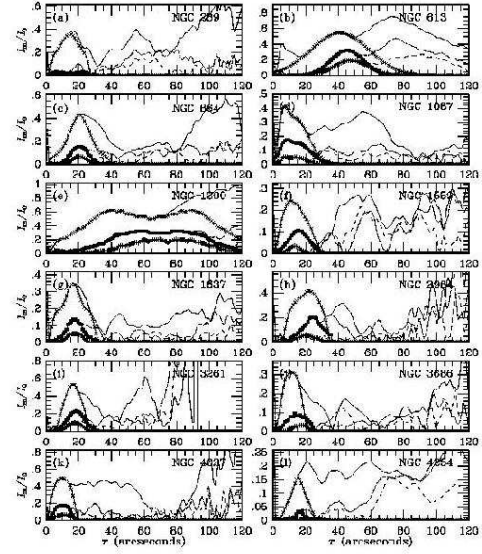


Fig. 2.—

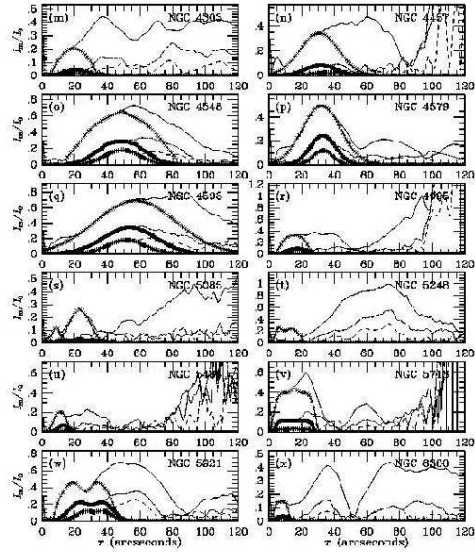


Fig. 2 (cont.).—

Fig. 2 (cont.).— Example plots of relative Fourier intensity amplitudes as a function of radius for 24 OSUBGS galaxies. Symbols show the extrapolations used for our analysis (see text). For each case, even terms for $m=2$ (solid curve), 4 (dotted curve), and 6 (short dashed curve) are shown.

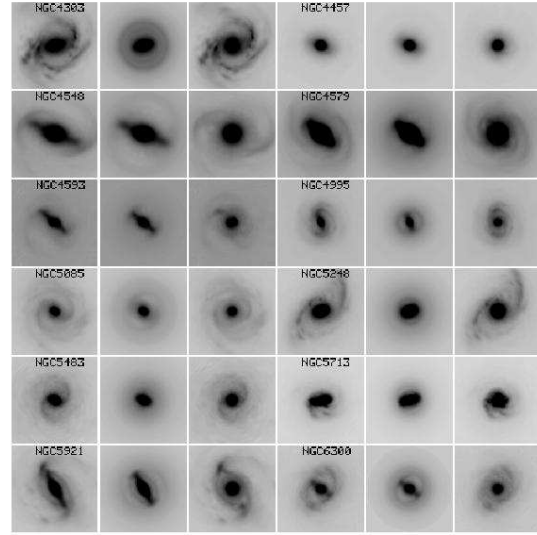
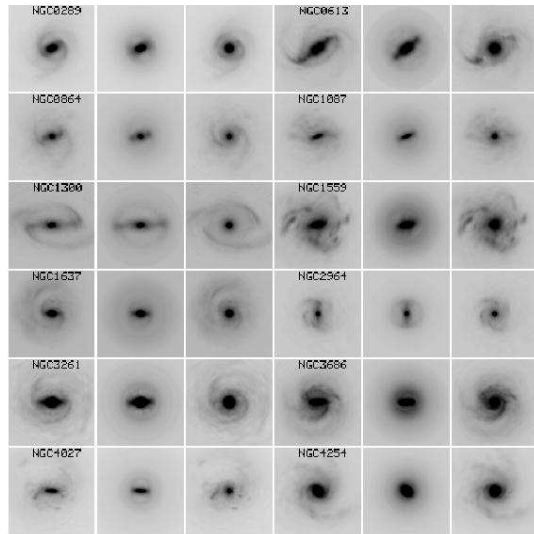


Fig. 3 (cont.).—

Fig. 3.—

Fig. 3 (cont.).— Illustration of the bar/spiral separations for the same 24 galaxies as in Figure 1, using the extrapolations shown in that figure. Three images are shown for each galaxy: the total $m=0$ -20 Fourier-smoothed image (left), the bar plus disk image (middle), and the spiral plus disk image (right).

Fig. 4.— Plots of maximum relative torques $Q_T(r)$ versus radius r for the bar and spiral of NGC 6951, from BBK03, illustrating the definitions of Q_b , Q_s , and Q_g and $r(Q_b)$, $r(Q_s)$, and $r(Q_g)$.

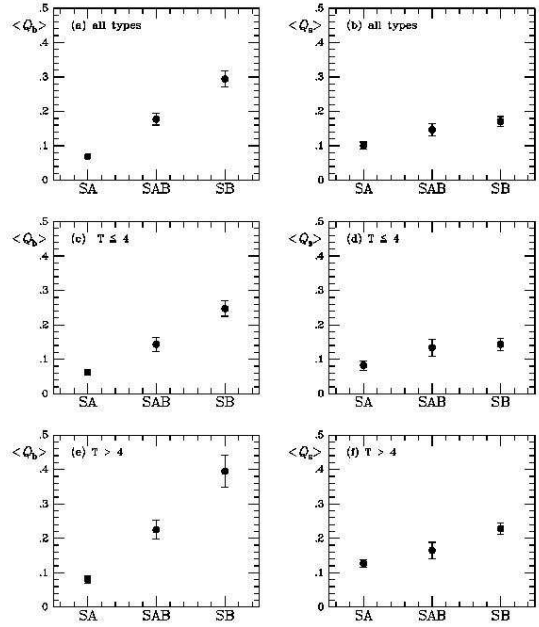
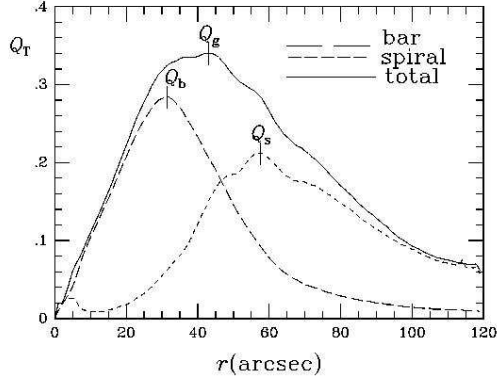


Fig. 5.— Plots of $\langle Q_b \rangle$ and $\langle Q_s \rangle$ for 146 OS-UBGS galaxies (excluding NGC 3646, classified as a ring galaxy in RC3): (a,b) over all spiral types; (c,d) for types at or earlier than Sbc ($T=4$); and (e,f) for types later than Sbc. The data illustrated are compiled in Table 2. The error bars are mean errors.

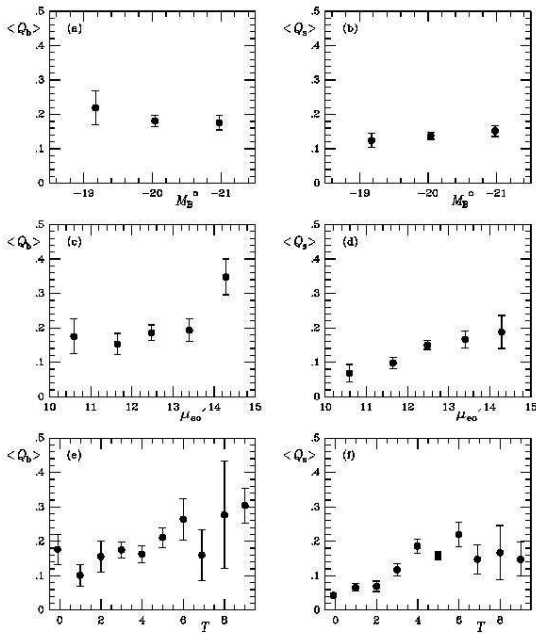


Fig. 6.— Plots of $\langle Q_b \rangle$ and $\langle Q_s \rangle$ as a function of: (a,b) absolute blue total magnitude M_B^o ($n=147$ galaxies); (c,d) photoelectrically determined mean effective surface brightness in RC3, corrected for tilt and Galactic extinction ($n=113$ galaxies); and (e,f) RC3 revised Hubble type index ($n=147$ galaxies). The error bars are mean errors.

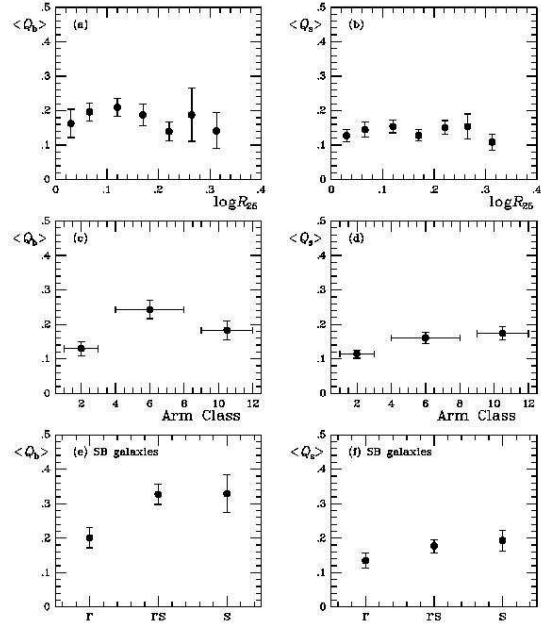


Fig. 7.— Plots of $\langle Q_b \rangle$ and $\langle Q_s \rangle$ as a function of: (a,b) RC3 logarithmic isophotal axis ratio at the $\mu_B=25.0$ mag arcsec $^{-2}$ surface brightness level ($n=144$ galaxies); (c,d) spiral Arm Class (Elmegreen & Elmegreen 1987; $n=107$ galaxies); and (e,f) SB spiral variety ($n=53$ galaxies).

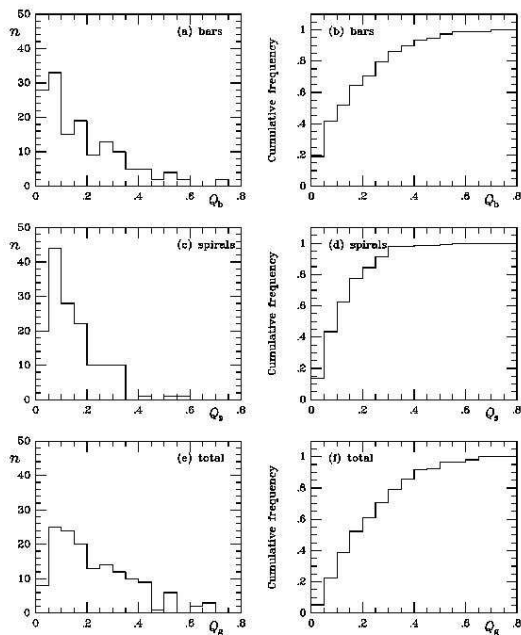


Fig. 8.— Histograms of the distributions of (a,b) bar strength Q_b , (c,d) spiral strength Q_s , and (e,f) total nonaxisymmetric strength Q_g , for 147 OSUBGS galaxies less inclined than 65° . The cumulative histograms are normalized to the total number of galaxies. The Q_g data are from LSBV04.

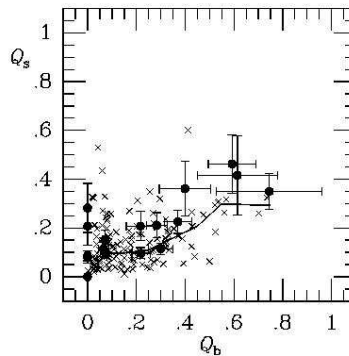


Fig. 9.— Plot of spiral strength Q_s versus bar strength Q_b for 147 OSUBGS galaxies (*crosses*) and 17 nearby spirals from Block et al. (2004; *filled circles*). The solid curve shows the median Q_s for steps of 0.1 in Q_b .